Light trapping in a polymer solar cell by tailored quantum dot emission

Yunlu Xu[1,2] and Jeremy N. Munday[1,2,*]

[1]*Department of Electrical and Computer Engineering, University of Maryland, College Park, Maryland 20740, USA*
[2]*Institute for Research in Electronics and Applied Physics, University of Maryland, College Park, Maryland 20740, USA*
[*]*jnmunday@umd.edu*

Abstract: We propose a polymer photovoltaic device with a new scattering mechanism based on photon absorption and re-emission in a quantum dot layer. A matrix of aluminum nanorods with optimized radius and period are used to modify the coupling of light emitted from the quantum dots into the polymer layer. Our analysis shows that this architecture is capable of increasing the absorption of an ordinary polymer photovoltaic device by 28%.

OCIS codes: (040.5350) Photovoltaic; (310.6628) Subwavelength structures, nanostructures.

References and links

1. C. J. Brabec, "Organic photovoltaics: technology and market," Sol. Energy Mater. Sol. Cells **83**(2–3), 273–292 (2004).
2. F. C. Krebs, S. A. Gevorgyan, and J. Alstrup, "A roll-to-roll process to flexible polymer solar cells: model studies, manufacture and operational stability studies," J. Mater. Chem. **19**(30), 5442 (2009).
3. F. C. Krebs, T. Tromholt, and M. Jørgensen, "Upscaling of polymer solar cell fabrication using full roll-to-roll processing," Nanoscale **2**(6), 873–886 (2010).
4. A. J. Medford, M. R. Lilliedal, M. Jørgensen, D. Aarø, H. Pakalski, J. Fyenbo, and F. C. Krebs, "Grid-connected polymer solar panels: initial considerations of cost, lifetime, and practicality," Opt. Express **18**(S3 Suppl 3), A272–A285 (2010).
5. H. Zhou, Y. Zhang, J. Seifter, S. D. Collins, C. Luo, G. C. Bazan, T.-Q. Nguyen, and A. J. Heeger, "High-Efficiency Polymer Solar Cells Enhanced by Solvent Treatment," Adv. Mater. **25**(11), 1646–1652 (2013).
6. J. You, L. Dou, Z. Hong, G. Li, and Y. Yang, "Recent trends in polymer tandem solar cell research," Prog. Polym. Sci. **38**(12), 1909–1928 (2013).
7. L. Dou, J. You, J. Yang, C.-C. Chen, Y. He, S. Murase, T. Moriarty, K. Emery, G. Li, and Y. Yang, "Tandem polymer solar cells featuring a spectrally matched low-bandgap polymer," Nat. Photonics **6**(3), 180–185 (2012).
8. O. Hagemann, M. Bjerring, N. C. Nielsen, and F. C. Krebs, "All solution processed tandem polymer solar cells based on thermocleavable materials," Sol. Energy Mater. Sol. Cells **92**(11), 1327–1335 (2008).
9. J. You, L. Dou, K. Yoshimura, T. Kato, K. Ohya, T. Moriarty, K. Emery, C.-C. Chen, J. Gao, G. Li, and Y. Yang, "A polymer tandem solar cell with 10.6% power conversion efficiency," Nat Commun. **4**, 1446 (2013).
10. W. Li, A. Furlan, K. H. Hendriks, M. M. Wienk, and R. A. J. Janssen, "Efficient Tandem and Triple-Junction Polymer Solar Cells," J. Am. Chem. Soc. **135**(15), 5529–5532 (2013).
11. J. You, C.-C. Chen, Z. Hong, K. Yoshimura, K. Ohya, R. Xu, S. Ye, J. Gao, G. Li, and Y. Yang, "10.2% Power Conversion Efficiency Polymer Tandem Solar Cells Consisting of Two Identical Sub-Cells," Adv. Mater. **25**(29), 3973–3978 (2013).
12. A. Luque and S. Hegedus, Handbook of Photovoltaic Science and Engineering. Wiley, 2003.
13. W. U. Huynh, J. J. Dittmer, and A. P. Alivisatos, "Hybrid Nanorod-Polymer Solar Cells," Science **295**(5564), 2425–2427 (2002).
14. L. Song and A. Uddin, "Design of high efficiency organic solar cell with light trapping," Opt. Express **20**(S5 Suppl 5), A606–A621 (2012).
15. W. E. I. Sha, W. C. H. Choy, Y. Wu, and W. C. Chew, "Optical and electrical study of organic solar cells with a 2D grating anode," Opt. Express **20**(3), 2572–2580 (2012).
16. S. Y. Chou and W. Ding, "Ultrathin, high-efficiency, broad-band, omni-acceptance, organic solar cells enhanced by plasmonic cavity with subwavelength hole array," Opt. Express **21**(S1 Suppl 1), A60–A76 (2013).
17. H. Shen, P. Bienstman, and B. Maes, "Plasmonic absorption enhancement in organic solar cells with thin active layers," J. Appl. Phys. **106**(7), 073109 (2009).
18. I. Kim, D. S. Jeong, T. S. Lee, W. S. Lee, and K.-S. Lee, "Plasmonic nanograting design for inverted polymer solar cells," Opt. Express **20**(S5 Suppl 5), A729–A739 (2012).

#198490 - $15.00 USD Received 30 Sep 2013; revised 28 Dec 2013; accepted 8 Jan 2014; published 23 Jan 2014

19. S. Mokkapati and K. R. Catchpole, "Nanophotonic light trapping in solar cells," J. Appl. Phys. **112**(10), 101101 (2012).
20. E. Stratakis and E. Kymakis, "Nanoparticle-based plasmonic organic photovoltaic devices," Mater. Today **16**(4), 133–146 (2013).
21. Q. Gan, F. J. Bartoli, and Z. H. Kafafi, "Plasmonic-Enhanced Organic Photovoltaics: Breaking the 10% Efficiency Barrier," Adv. Mater. **25**(17), 2385–2396 (2013).
22. Z. Ye, S. Chaudhary, P. Kuang, and K.-M. Ho, "Broadband light absorption enhancement in polymer photovoltaics using metal nanowall gratings as transparent electrodes," Opt. Express **20**(11), 12213–12221 (2012).
23. K. Q. Le, A. Abass, B. Maes, P. Bienstman, and A. Alù, "Comparing plasmonic and dielectric gratings for absorption enhancement in thin-film organic solar cells," Opt. Express **20**(S1), A39–A50 (2012).
24. V. E. Ferry, J. N. Munday, and H. A. Atwater, "Design Considerations for Plasmonic Photovoltaics," Adv. Mater. **22**(43), 4794–4808 (2010).
25. H. A. Atwater and A. Polman, "Plasmonics for improved photovoltaic devices," Nat. Mater. **9**(3), 205–213 (2010).
26. B. Yu, S. Goodman, A. Abdelaziz, and D. M. O'Carroll, "Light-management in ultra-thin polythiophene films using plasmonic monopole nanoantennas," Appl. Phys. Lett. **101**(15), 151106 (2012).
27. A. J. Nozik, "Quantum dot solar cells," Physica E **14**, 115–120(2002).
28. Y.-J. Lee, Y.-C. Yao, M.-T. Tsai, A.-F. Liu, M.-D. Yang, and J.-T. Lai, "Current matching using CdSe quantum dots to enhance the power conversion efficiency of InGaP/GaAs/Ge tandem solar cells," Opt. Express **21**(S6), A953–A963 (2013).
29. C. Cheng and X. Wang, "A Comparative Study of Spectral Characteristics of CdSe and CdSe/ZnS Quantum Dots" International Symposium on Biophotonics, Nanophotonics and Metamaterials, 2006. Metamaterials, 366–369 (2006).
30. The experimental absorption data (A.U.) was obtained from solution and has been converted into absorption (%) using typical k values for bulk.
31. J. N. Munday and H. A. Atwater, "Large integrated absorption enhancement in plasmonic solar cells by combining metallic gratings and antireflection coatings," Nano Lett. **11**(6), 2195–2201 (2011).

1. Introduction

Photovoltaic devices offer an appealing alternative to fossil fuel-based energy sources; however, the cost-per-Watt of solar power in many regions is prohibitively high, resulting in a need for low-cost photovoltaics concepts. To this end, polymers have become an attractive alternative to traditional inorganic semiconductors due to their low-cost and ease of fabrication [1–4]. Despite these benefits, polymer photovoltaics have been hindered by their relatively low efficiencies [5] when compared to traditional, inorganic cells. Ineffective absorption and carrier collection results in a decrease of both the short circuit current and the open circuit voltage.

Many routes have been taken to improve the solar conversion efficiencies of polymer solar cells. One option for improving the voltage is the development of tandem polymer cells [6–8]. These devices typically consist of two or three junctions configured in a tandem fashion, which allows for the summation of their voltages, hence resulting in increased power output [9–11]. However, this process adds complexity to the fabrication process due to the requirement of tunnel junctions and current matching conditions throughout the device [12].

In order to increase the generated current in an optically thin cell, higher absorption is needed within the polymer. This can be achieved through the use of surface texturing, nanostructing, plasmonics, or other light trapping architectures [13–26].

Here, we proposed a new mechanism for increasing the efficiency of polymer solar cells through the use of quantum dot (QD) scatterers. QDs are widely used in photovoltaic applications either as the traditional active layer or to generate multiple excitons from a single incident photon [27]. Recently, QDs have also been used to modify the incoming spectrum for tandem devices to improve the current matching conditions for such devices [28]. Rather than focusing on multiple carrier generation or modification of the spectrum, we describe the use of QDs to change the directionality of the incident photons to improve coupling to the nearby photoactive layer. High lumenescence QDs can absorb photons that are transmitted through the photoactive polymer layer and then re-emit photons back into waveguide modes of the structure, which can be absorbed with high probability within the active polymer layer.

#198490 - $15.00 USD Received 30 Sep 2013; revised 28 Dec 2013; accepted 8 Jan 2014; published 23 Jan 2014

Unlike the traditional usage of QDs for multi-exiton generation or intermediate band solar cells, we use quantum dots as scatterers to boost the absorption within a thin active layer of the cell. We further introduce nanorod structures surrounding the QDs to allow for current collection from the polymer. These nanorods also enable control of the coupling of the incident light to the polymer and of the QD emission into waveguide modes within the device, which can further increase the absorption.

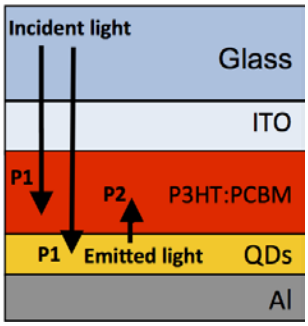

Fig. 1. Schematic of the polymer cell and simulation procedure. Light is incident from the glass, and useful absorption during the first path (P1) occurs in both the polymer (P3HT:PCBM) and within the QD layer. The QDs will emit photons with a particular probability resulting in a second path (P2) through the cell, which can be absorbed in the polymer.

2. Modeling

In order to determine the generated photocurrent, we calculate the absorption, emission, and re-absorption rates within the various layers of our structure (Fig. 1). The calculation proceeds as follows. First, Maxwell's equations are solved numerically using the Finite Difference Time Domain method (Lumerical FDTD Solutions) for the structure shown in Fig. 1. In this first part, the QDs are treated simply as an absorbing layer described by a complex index of refraction. The number of photons absorbed in both the polymer layer, $N_{poly}(\lambda)$, and in the QD layer, $N_{QDS}(\lambda)$, due to the injection of a plane wave source is calculated [24]. In the second part, we simulate the re-emission of the QDs. The QDs are treated as dipole sources that are distributed uniformly, and the emission spectrum is described by a Gaussian function, $\mathcal{D}(\lambda)$, peaked at the emission wavelength. For a typical simulation, 1080 dipoles per unit volume (thickness times the period squared) are used, and the strength of each dipole is weighed by the local absorption due to plane wave injection. During the emission simulation, the dipole is assumed to be surrounded by a dielectric slab, whose index of refraction is completely real. This assumption restricts further absorption within the QD layer; however, as we show in the following sections, the QDs typically emit into modes with weak overlap with the QD layer. We define the absorptance of the re-emitted photons within the polymer layer, $A_{2nd}(\lambda)$, as the ratio of the number of absorbed photons to the number of emitted photons from the dipole sources. The total number of absorbed photons within the polymer due to both processes is:

$$N_{tot} = \int_{\substack{solar\\spectrum}} N_{poly}(\lambda)d\lambda + \int_{\substack{emission\\spectrum}} \left\{ D(\lambda)A_{2nd}(\lambda)\left[\int_{\substack{solar\\spectrum}} N_{QDs}(\lambda')d\lambda' \right] \right\} d\lambda. \quad (1)$$

The QDs are modeled after experimental data from CdSe quantum dots [29]. In order to obtain the refractive index of the QD layer, we treat the layer as a bulk material and calculate the refractive index from $n = \sqrt{\mu\varepsilon}$. With $\mu = 1$, we use a Drude-Lorentz model to calculate the electrical permittivity, ε. Using the Beer-Lambert law, we compare the calculated

#198490 - $15.00 USD Received 30 Sep 2013; revised 28 Dec 2013; accepted 8 Jan 2014; published 23 Jan 2014

absorption spectrum of a 3 nm thick layer of CdSe QDs with experimental data [29]. Figure 2 shows the refractive index used for the simulations is in good agreement with the experimental absorption data [30].

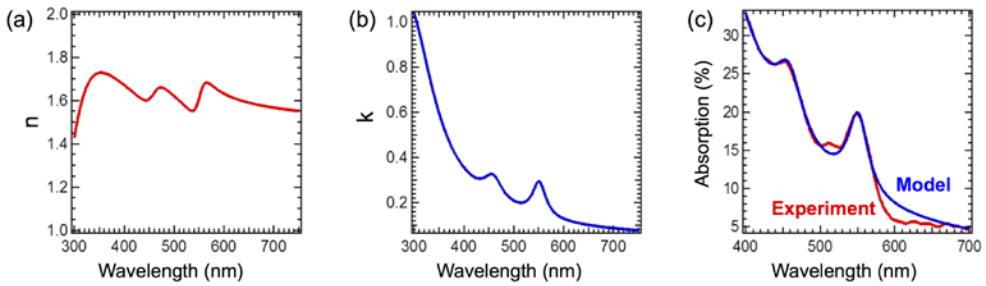

Fig. 2. The (a) real and (b) imaginary parts of the refractive index of the quantum dots used in our model. (c) Comparison of absorption spectrum of the quantum dots in the model (blue) to the experimental data (red) shows good agreement.

3. Results

Following the calculation procedure described above for a simple planar structure (Fig. 1), we find that the expected photocurrent is enhanced by 29.4% when the QD layer is present compared to the same structure without the QD layer (5.31×10^{20} photons absorbed). 5.8% of the enhancement is due to absorption in the polymer as a result of the emission of the QDs, and the rest of enhancement results from thin film interference effects that occur due to the addition of the QD layer. Despite the relatively large expected photocurrent generation, photocurrent collection would be difficult for the structure of Fig. 1. Because the QDs are acting predominantly as optical scattering structures, an additional conduction path is needed for carriers generated within the polymer. To solve this problem, aluminum nanorods are inserted between the polymer and the aluminum contact to allow electrical conductivity to the back contact, as is shown in Fig. 3.

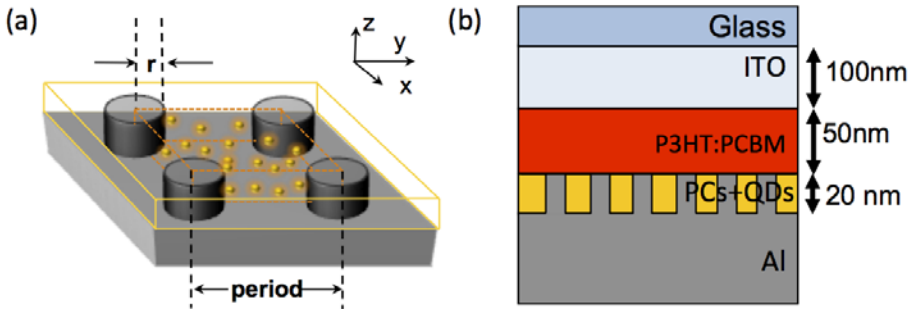

Fig. 3. (a) Schematic diagram of the aluminum nanorod layer filled with uniformly distributed quantum dots (orange) and (b) cross section of the entire solar cell structure. The orange dotted box in (a) is the simulated unit volume, which contains 1080 dipoles.

We repeat the simulation procedure outlined in Section 2 for a nanorod array with a period of 220 nm and a nanorod radius of 70 nm. The photons absorbed in the polymer and QD layers are 6.44×10^{20} and 0.52×10^{20}, respectively, during the first simulation. The re-emission from the QDs results in 0.04×10^{20} photons being absorbed during the second step of the simulation. Surprisingly, the total number of photons absorbed in the polymer is 6.48×10^{20}, which is slightly lower than the result obtained from the structure without nanorods. This is the result of inefficient coupling between the incoming light and the structure as well as poor coupling between the QD emission and the polymer absorption.

#198490 - $15.00 USD Received 30 Sep 2013; revised 28 Dec 2013; accepted 8 Jan 2014; published 23 Jan 2014

Optimization. In order to improve the absorption and coupling, a parameter sweep of the radius and period is performed. This optimization process is depicted in Fig. 4. The first path absorption shows increased absorption in the polymer layer for large periods and increased absorption in the QD layer for short periods and small radii [Figs. 4(a) and 4(b)]. Absorption in the aluminum nanorods increases for short periods and large radii due to the increased fraction of metal in the layer containing QDs [Fig. 4(c)]. Thus, it is important to reduce the metal fraction in order to avoid ohmic loss. Figure 4d shows that the coupling efficiency (i.e. the ratio of the number of photons absorbed in the polymer layer due to quantum dot emission to the number of photons emitted by the QDs) is fairly uniform (second path absorption); however, optimal points are found where the emission is coupled more efficiently into the polymer layer rather than out of the cell or into the surrounding metal.

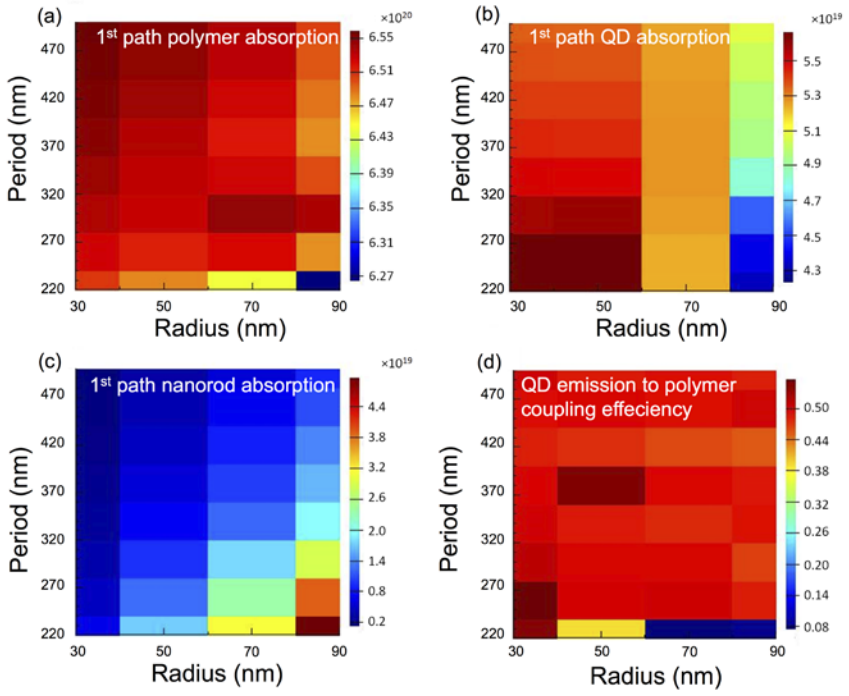

Fig. 4. The number of photons absorbed in (a) the polymer, (b) the QD layer, and (c) the aluminum nanorods during the first path. (d) The coupling efficiency of the emitted photons from the QDs to the polymer layer.

Because the final absorption consists of two parts (initial absorption in the polymer and secondary absorption in the polymer from QD emission), there is a trade-off between these parameters. Figure 5 shows the total number of absorbed photons in the polymer after the entire calculation. Although the total number of photons absorbed depends on both the radius and the periodicity of the array, the overall absorption is relatively insensitive to the exact value of the radius and period for periods in the range of 260 to 500 nm and for radii in the range of 30 to 70 nm. It is possible to couple to both localized and propagating surface plasmon modes by changing the period and radius of the rods [31]; however, the overall absorption is relatively insensitive to these changes for the structure under consideration. The highest value of absorption occurs in the structure with nanorods of 30 nm radius and 260 nm period. This is because the loss in the aluminum is relatively low in nanorods with smaller radii. The total number of photons absorbed in the polymer is 6.84×10^{20}, which has a 28.6% enhancement, and one fifth of the enhancement (6%) comes from the emission of the QDs.

#198490 - $15.00 USD Received 30 Sep 2013; revised 28 Dec 2013; accepted 8 Jan 2014; published 23 Jan 2014

The photocurrent enhancement in this structure is comparable to that of the planar structure; however, there is now a conduction path for carrier collection.

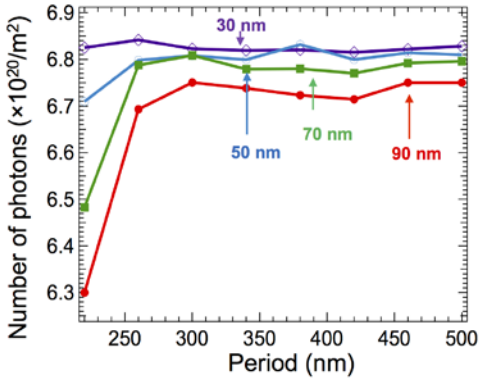

Fig. 5. Total number of photons absorbed in the polymer for different radii and periods of the nanorod array (including the absorption from the emission of QDs). The radii are 30 nm (purple), 50 nm (blue), 70 nm (green), 90 nm (red).

4. Discussion

Because the inclusion of a QD layer can lead to absorption enhancements either through modifying the initial absorption or through the reemission process, it is necessary to consider both effects in further detail.

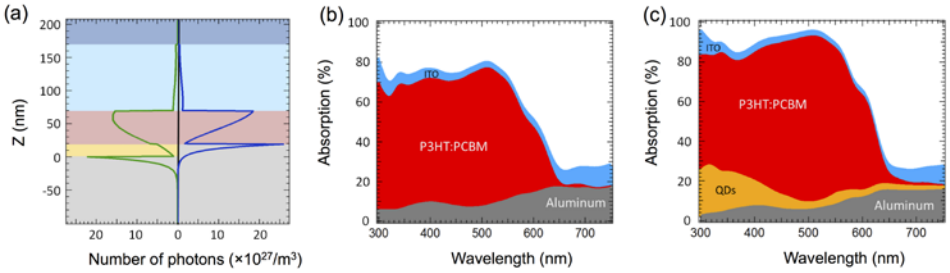

Fig. 6. Absorption comparison during the first path for the traditional polymer cell and the QD enhanced polymer cell. (a) Cross section showing the number of absorbed photons per cubic meter with (green solid line) and without (blue solid line) the QD layer. (b) The absorption in each layer of the ordinary polymer cell. (c) The absorption in each layer of our QD enhanced polymer cell. The absorption in the QDs occurring for λ>600 nm will not contribute to the re-emission process because they do not contain sufficient energy to cause emission.

By adding the QD layer to the structure, we find that the peak in the number of absorbed photons moves toward the middle of the polymer layer instead of staying on the top boundary, as is shown in Fig. 6(a). Figure 6(c) shows that the absorption enhancement occurs over almost the entire polymer region, when compared to Fig. 6(b). In addition, because the QDs absorb a certain fraction of the energy that would otherwise be lost to absorption within the aluminum [compare Figs. 6 (b) and (c)], this energy has the possibility of being recovered through the re-emission process. Further, because the QD emission allows for a second absorption path for photons in the polymer, this process leads to an additional enhancement, as can clearly be seen in Fig. 7. Interestingly, the absorption around 559 nm reaches 100% even though the QD to polymer coupling efficiency is less than 100%. This is due to fact that photons emitted at 559 nm could have resulted from the absorption of photons of a different wavelength. Thus, because there are more 559 nm photons available after emission than there were from the initial spectrum, the absorption could in principle exceed 100% at a particular

#198490 - $15.00 USD Received 30 Sep 2013; revised 28 Dec 2013; accepted 8 Jan 2014; published 23 Jan 2014

wavelength. If the QDs do not have 100% fluorescence efficiency, the peak absorption is reduced, as shown in Fig. 7.

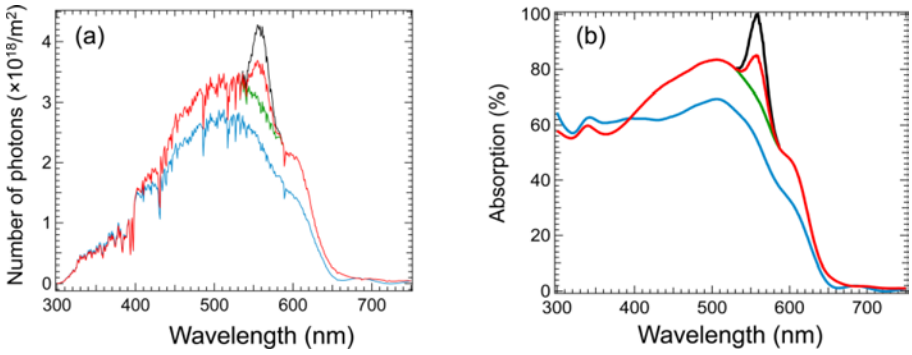

Fig. 7. The comparison of absorption spectra of the polymer (blue) and the QD enhanced polymer (Green: without QD emission, Red: with 50% QD emission, Black: with 100% QD emission) cells without the nanorod array. (a) The absorbed number of photons as a function of wavelength under AM 1.5G solar illumination. (b) The percentage of photons absorbed compared to the incident solar illumination. Note: the peak at ~560 nm results from the absorption of photons emitted from the QDs and could in principle exceed 100% due to the redistribution of higher energy photons. The radius and period of the nanorods are 30 nm and 260 nm, respectively.

To explain the increased absorption, we note that the QDs can emit into waveguide modes of the structure. Here we consider the waveguide modes that exist within the planar structures at a wavelength of 559 nm, which corresponds to the emission peak of the QDs. Our simulations show that two modes can exist in the structures with or without the QD layer: transverse electric (TE) and transverse magnetic (TM). The normalized electric field intensities of the TE and TM modes are depicted in Fig. 8.

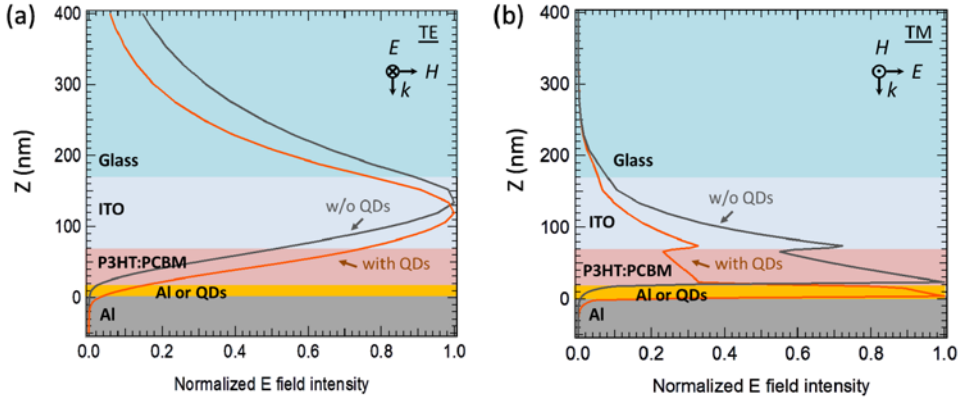

Fig. 8. Electrical field intensity of fundamental (a) TE and (b) TM modes in the solar cell. Orange and gray lines are the field intensities for structures with and without quantum dots, respectively. The layers are depicted on the background: glass (blue), ITO (light blue), polymer (red), QDs (yellow), and aluminum (gray); note: for the structure without QDs, the yellow layer is aluminum. The analysis is performed at the emission peak of QDs (i.e. 559 nm).

To determine whether or not the QDs can emit efficiently into the guided modes of the structure, we determine the electric field intensity created by a dipole positioned in the center of the QD layer. Figure 9 shows that the field profiles, as determined 100 nm from the dipole in the X-Y direction, are very similar to the fundamental modes of the structure. This

#198490 - $15.00 USD Received 30 Sep 2013; revised 28 Dec 2013; accepted 8 Jan 2014; published 23 Jan 2014

correspondence indicates that the QDs emit efficiently into either TE or TM modes depending on the dipole orientation. Because the dipole orientation is random, it is more likely for the

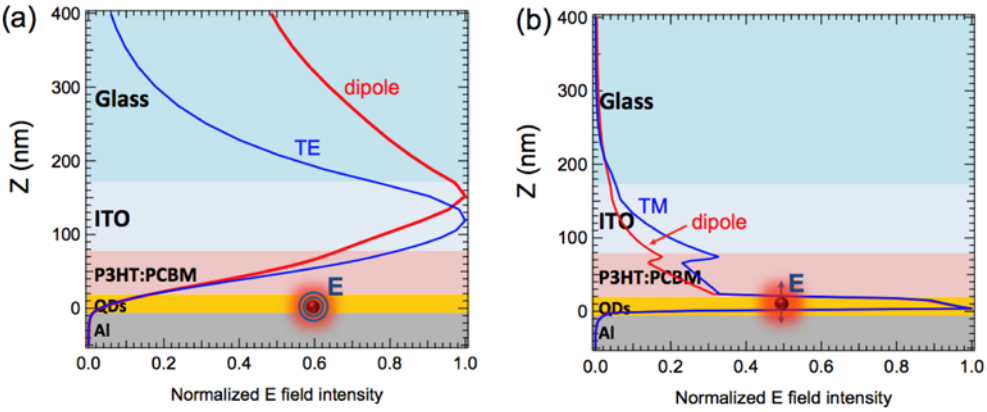

Fig. 9. The coupling of dipole emission into the waveguide mode of the solar cell. Blue data are fundamental (a) TE and (b) TM modes, and red data are the field intensities resulting from dipole emission. The layers are depicted on the background: glass (blue), ITO (light blue), polymer (red), QDs (yellow) and aluminum (gray).

dipoles to emit into the TE mode due to the symmetry of this 2-D structure. This result also suggests that our assumption of weak secondary absorption in the QD layer due to QD emission is valid.

Although we have focused on a 50 nm thick polymer layer to ensure collection of generated carriers, the enhancement persists for a range of thicknesses (Fig. 10). As the thickness increases more photons are absorbed by the polymer layer, leaving fewer photons to be absorbed by the QDs. As a result, the absorption due to QD emission becomes smaller. The effect of the QDs is most pronounced for polymer thicknesses below 80 nm. For thicker films the interference conditions change for the first pass absorption, and the structure without quantum dots performs better for polymer thicknesses from 80 to 140 nm. For thicker films, the QDs again improve the performance; however, charge collection becomes more critical to the design for these thicker films.

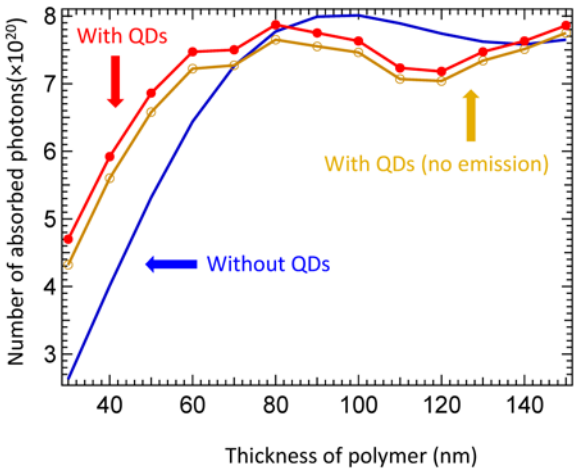

Fig. 10. The number of absorbed photons is influenced by the thickness of the polymer layer. The structure with quantum dots outperforms the structure without quantum dots for polymer thicknesses below 80 nm. For thicker films, there is a tradeoff between carrier collection and thin-film interference effects.

#198490 - $15.00 USD Received 30 Sep 2013; revised 28 Dec 2013; accepted 8 Jan 2014; published 23 Jan 2014

5. Conclusion

In conclusion, we have shown that a new method, using QDs as scatters, has the ability to increase the absorption in a polymer layer of an organic solar cell while simultaneously reducing the loss in the aluminum contact layer, thus increasing the efficiency of the polymer solar cell. Further, the emission from the QDs can be coupled into waveguide modes of the structure, which leads to the largest enhancements. There are two possible modes that exist within these thin cells, and the TE mode plays the most important role in determining the absorption performance. While the results presented here pertain to polymer solar cells, these concepts can be extended to other photovoltaic systems, detectors, or sensors.

Acknowledgment

The authors acknowledge partial financial support for this project from a Minta Martin Research Award and the University of Maryland.

#198490 - $15.00 USD Received 30 Sep 2013; revised 28 Dec 2013; accepted 8 Jan 2014; published 23 Jan 2014